Supporting Information:

Rapid Aqueous-phase Photooxidation of Dimers in α-Pinene SOA

Ran Zhao[1,ǂ*], Dana Aljawhary[1,*], Alex K.Y. Lee[1,±], and Jonathan P.D. Abbatt[1]

[1] Department of Chemistry, University of Toronto, Toronto, ON, Canada, M5S 3H6.

[ǂ] Now at: Division of Chemistry and Chemical Engineering, California Institute of Technology, Pasadena, CA, USA, 91801.

[±] Now at: Department of Civil and Environmental Engineering, National University of Singapore, Singapore, 117576.

* Correspondence: rzhao@caltech.edu, Tel: 1-626-395-9043

S1. Positive Matrix Factorization (PMF) Analysis

The PMF analysis extracts "factors" from temporally and chemically resolved data by categorizing species correlated in time.[1] In recent years, PMF analyses have been employed widely for aerosol mass spectrometry (AMS) data for source apportionment of ambient aerosol. Application of PMF analyses to laboratory experiments is less common[2] but is valuable for complex chemical systems such as in this work where species-resolved information is challenging to use when following multi-generational chemistry. PMF analyses were performed using the University of Colorado PMF Execute Calc Tool v.2.6. The analyses were performed only on the results of the iodide experiments, as iodide exhibits relatively uniform detection sensitivity towards multifunctional organic compounds that establish sufficient H-bonding with iodide (i.e., dimeric compounds).[3] The PMF analysis was applied to the unit mass resolution data, as unambiguous peak fitting for all the dimeric compounds is infeasible.

The optimal PMF result was achieved when three factors (p = 3) are applied, as judged from the optimization function (Q) of the PMF analysis. As shown in Figure S1, the change in the ratio of $Q/Q_{expected}$ is minimal between p = 3 and 4, indicating that applying four factors no longer significantly improves the solution of the PMF analysis. The time profiles of the three factors are shown in Figure S2a, with each time profile normalized to its maximum value. Based on the time profiles, the three factors are interpreted as the precursors (Factor 1), the 1st generation products (Factor 2), and the 2nd and later generation products (Factor 3). The mass spectra of the three factors are shown in Figure S2b, with the dimer regions magnified and shown in the insets. The two major peaks appearing in Factor 1 are m/z 299 and 313, corresponding to the iodide clusters of norpinic acid and pinic acid, respectively. These compounds are well established products arising in α-pinene ozonolysis.[4] The dimeric compounds are also captured by Factor 1 (Figure S2b). The relative contribution of precursors and dimeric compounds to Factors 2 and 3 is increasingly smaller, with the relative contribution of smaller products increasing. The PMF results provide additional and unique evidence that dimeric compounds are photooxidized in the aqueous phase, giving rise to monomeric products. More specifically, as mentioned in the main body of the paper, when the first-order rate constant for decay of Factor 1 is combined with our estimate of the OH concentration in the solution, an estimate of the second-order rate constant for decay of Factor 1 is obtained: 3.1×10^9 M^{-1} s^{-1}

To our best knowledge, this work demonstrates the first application of the PMF analysis to laboratory CIMS data, which is fundamentally different from AMS data. Therefore, one needs to be cautious in interpreting the factors. AMS employs heating and electron impact (EI) ionization which result in significant fragmentation of organic molecules.[5] Most peaks in the AMS spectra represent a fragment arising from numerous organic species, and the AMS PMF analysis indicates the mass fraction of the fragment

attributable to each extracted factor. On the other hand, CIMS is a soft ionization technique, and each CIMS peak likely represents an individual species and its structural isomers. As we applied the unit mass resolution data to the PMF analysis, each peak can potentially be comprised of multiple molecules with a same nominal mass. The CIMS PMF factors in the current work can be interpreted as a statistical description of the relative contribution of isobaric compounds in each nominal mass to the extracted factors. The CIMS data are also not as quantitative as the AMS data, as the CIMS sensitivity is not uniform across all the species.[3] A quantitative argument for the relative contribution of each CIMS PMF factor can be difficult.

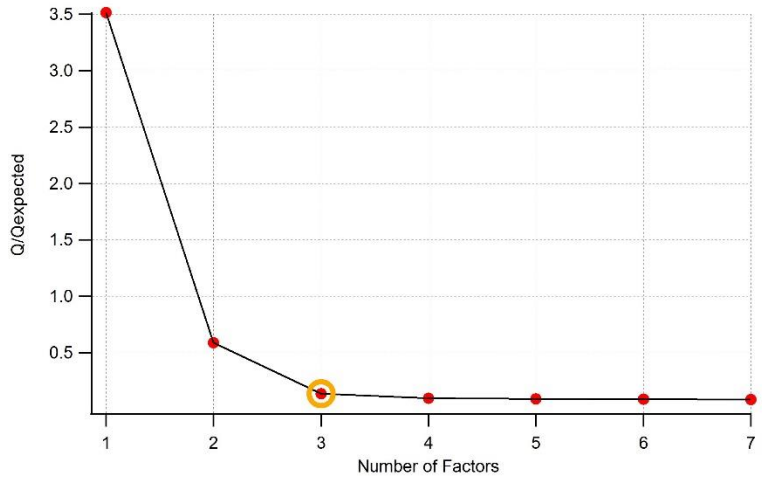

Figure S1: The ratio of $Q/Q_{expected}$ as a function of the number of factors. The optimal number of factors is indicated by the circle.

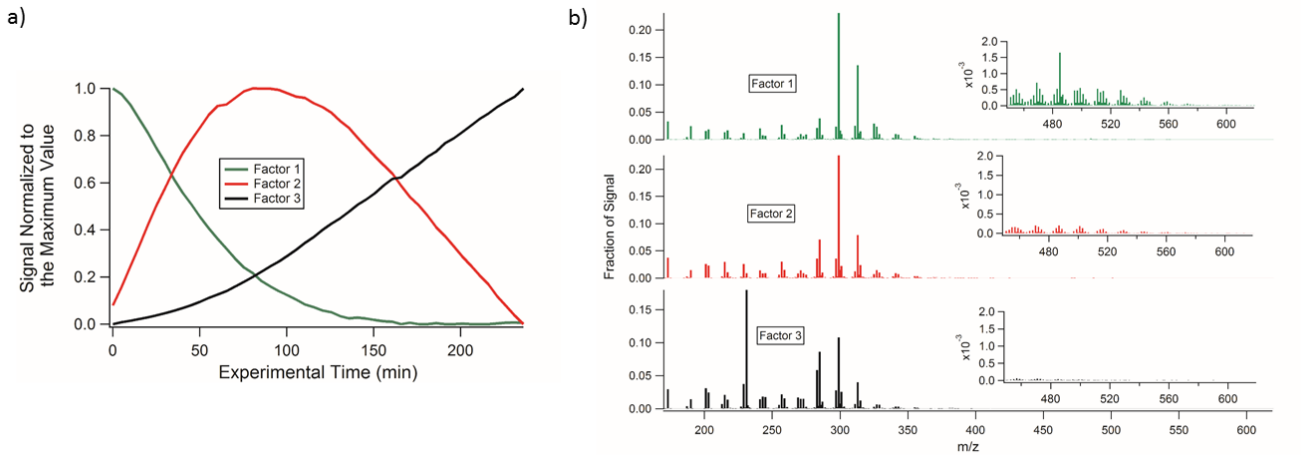

Figure S2: The time series of the three factors resulted in the PMF analysis of the iodide experiment (b). Each factor has been normalized to its maximum intensity. The mass spectrum of each factor is shown in (b). The dimer region of each spectrum is magnified and shown in the inset.

S2. Additional Information for OH Oxidation of Dimeric Compounds

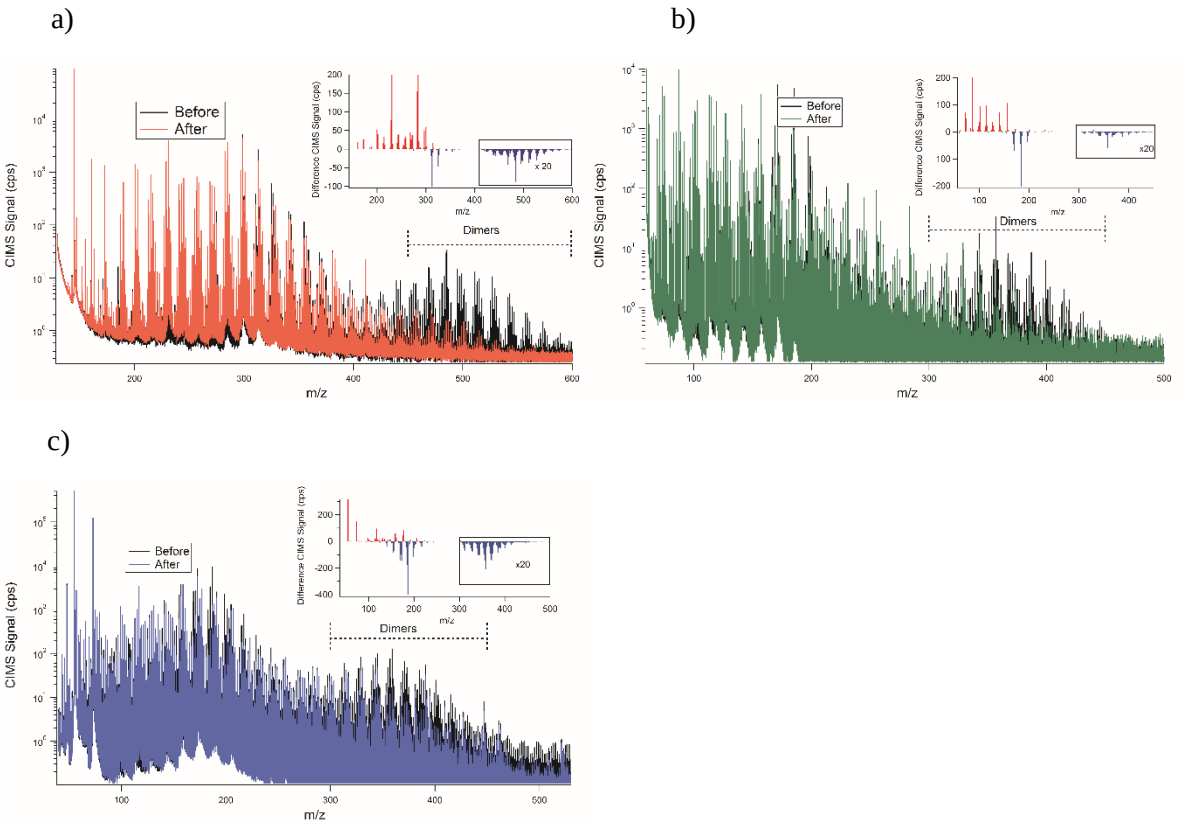

Figure S3: Mass spectral change observed during OH oxidation experiments employing a) the iodide, b) acetate and c) the water clusters reagent ions. Data from Aljawhary et al.[6] have been reanalyzed to emphasize the spectral changes in the dimeric region. Mass spectra at the beginning and the end of the experiment are shown by different colors, with the insets showing the differential mass spectra between the two. The mass spectral region arising from dimeric substances is indicated.

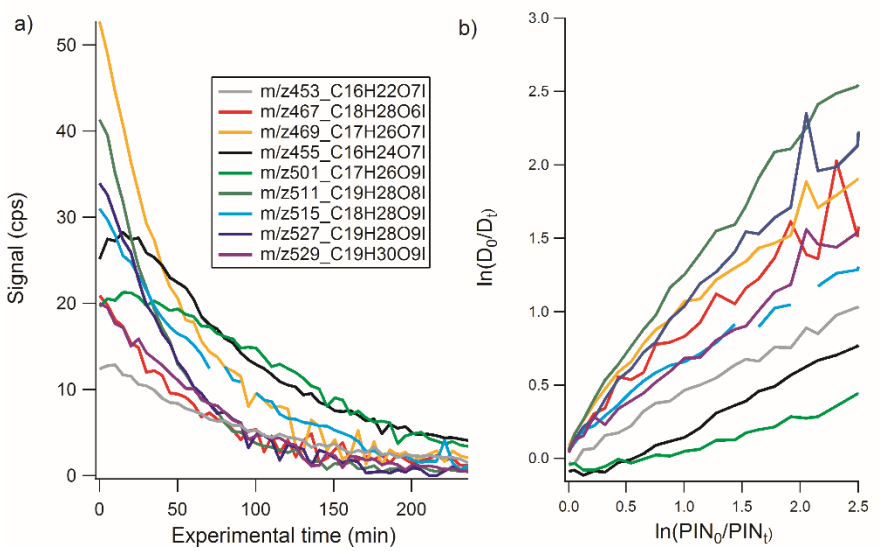

Figure S4: The time profiles (a) and relative kinetics plots (b) of the 9 dimeric compounds that are not presented in the main article. The data are obtained from the iodide OH oxidation experiment.

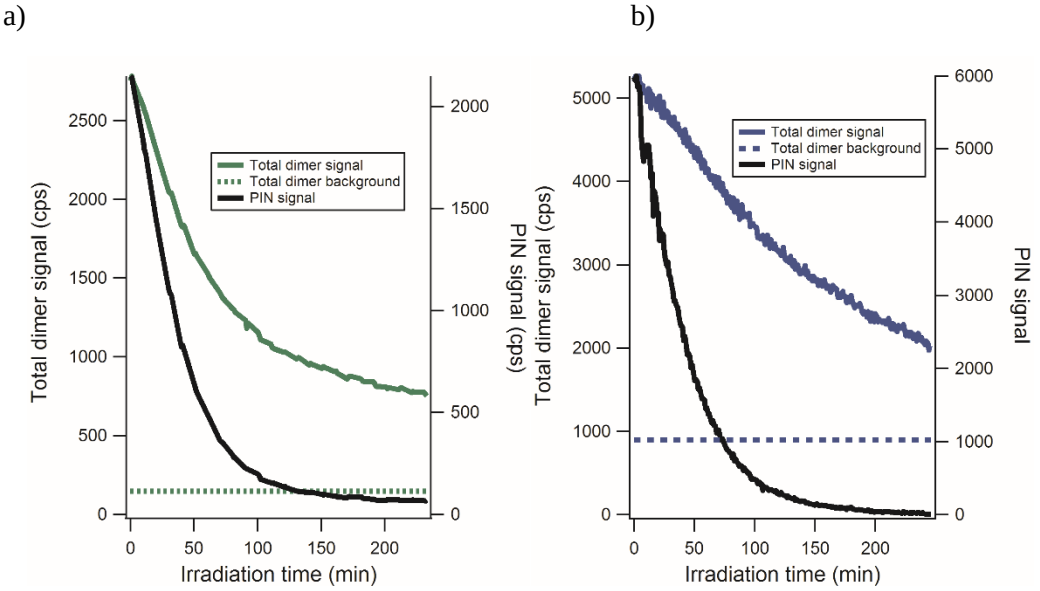

Figure S5: The decay of the total dimer signal and pinonic acid (PIN) signal observed during the a) acetate and b) water clusters experiments. The background of the total dimer signals is shown by the dashed lines.

S3. Probing the Mechanism of Dimer OH Oxidation

S3.1. Relative Reactivity of Hydrogen Atoms on Pinyl-diaterpenyl Ester

A structure-activity relationship (SAR) has been developed by Monod and Doussin[7,8] for aqueous-phase OH oxidation. While this SAR has been validated with a large number of small organic compounds, its applicability to dimeric compounds has not been examined. Particularly, the current version of the SAR is not compatible with compounds containing functional groups such as esters and peroxides. The SAR also requires an unambiguous molecular structure which is unavailable for most of the dimers in α-pinene SOA.

Here, we have employed the SAR to analyze the relative reactivity of hydrogens located on one example dimer, pinyl-diaterpenyl ester ($C_{17}H_{26}O_8$) whose structure has been confidently determined.[9] This analysis provides tentative clues to the most likely reaction mechanism. The structure of this dimer is shown in Figure S6a, with hydrogens at each location assigned a unique number. The SAR has been employed to calculate the OH reactivity of hydrogen(s) on each location, and the results are shown in Figure S6b.

Assumptions made for the calculations include: 1) the hydrogens on the carboxyl groups are much less reactive and hence can be neglected; 2) the ester group is considered as a hydroxyl group adjacent to a carbonyl group (ester is not considered in the SAR developed by Monod and Doussin); and 3) acid dissociation does not occur, with all the carboxylic acid remaining protonated. According to the calculation, the most reactive hydrogens are those on the four-membered ring (location 6, 8) and the two methyl groups attached immediately to the ring (location 7-1 and 7-2). The carbonyl group and carboxylic groups are strongly electron-withdrawing, and significantly deactivate hydrogens that are located on the α- or β-locations to these functional groups.

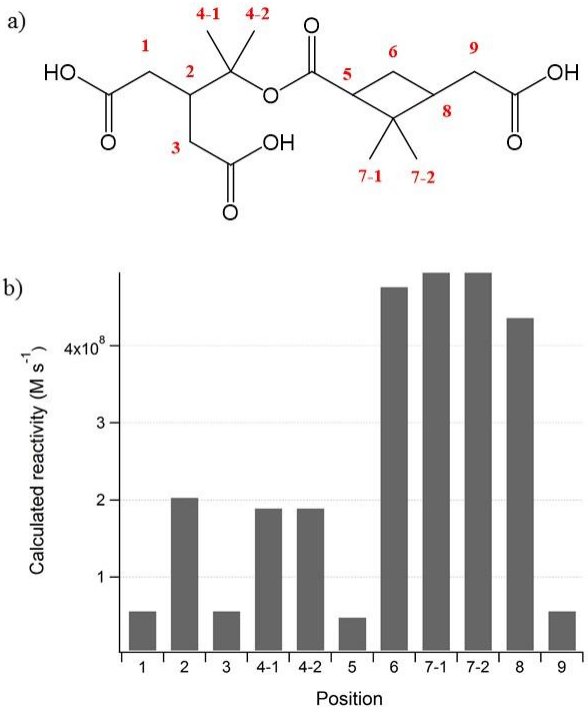

Figure S6: The structure of pinyl-diaterpenyl ester (a) with hydrogen(s) on each location assigned a unique number. The calculated OH reactivity of hydrogen(s) at each location (b) using the SAR developed by Monod and Doussin.[7,8]

S3.2. Fragmentation Reactions of Dimers

We have performed three case studies for pinyl-diaterpenyl ester, investigating H-abstraction at position 6, 7 and 8 (Figure S6.), respectively. These reactions result in fragmentation of the dimer, forming three distinct monomeric products (Figure S7). The Aerosol-CIMS signals of these three monomers (m/z corresponding to the iodide cluster of these compounds) are traced and are shown in Figure S8. Figure S8 shows that these monomers indeed form to different extents during the OH oxidation experiment. We note that the OH oxidation mechanism is highly complex, with multiple possible reaction pathways. Each of the case studies here is intended to present one example reaction pathway which leads to one of the many possible monomeric compounds. Although the high mass resolution data for these compounds are shown here, each of the elemental compositions can be comprised of more than one isobaric compounds. For example, the signal of C5H6O4I exhibits a second rise towards the latter half of the experiment (Figure S8), indicating that either multiple compounds are responsible for this m/z or multiple reaction mechanisms are giving rise to this compound.

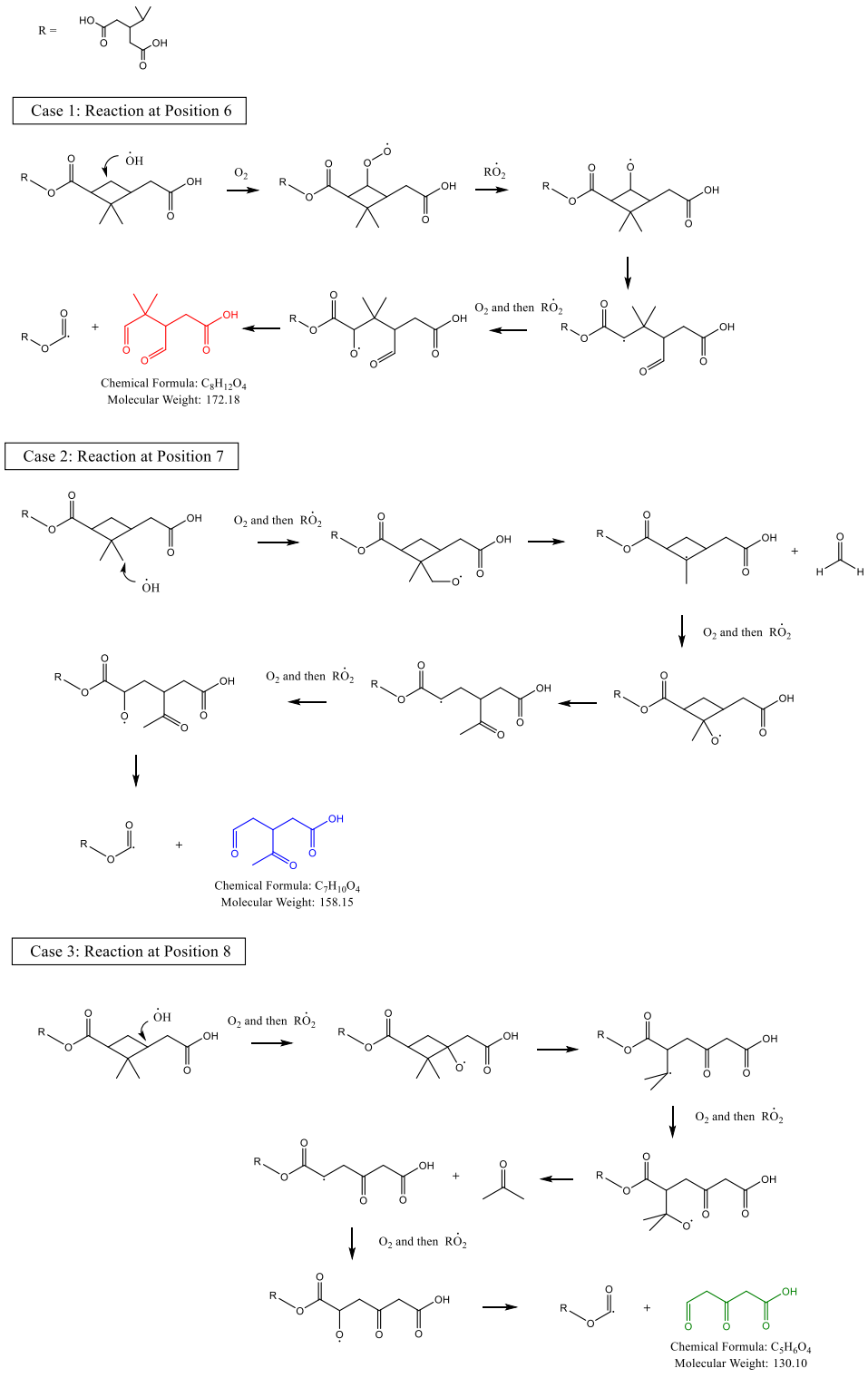

Figure S7: Three case studies for likely reaction mechanisms of the OH oxidation of pinyl-diaterpenyl ester.

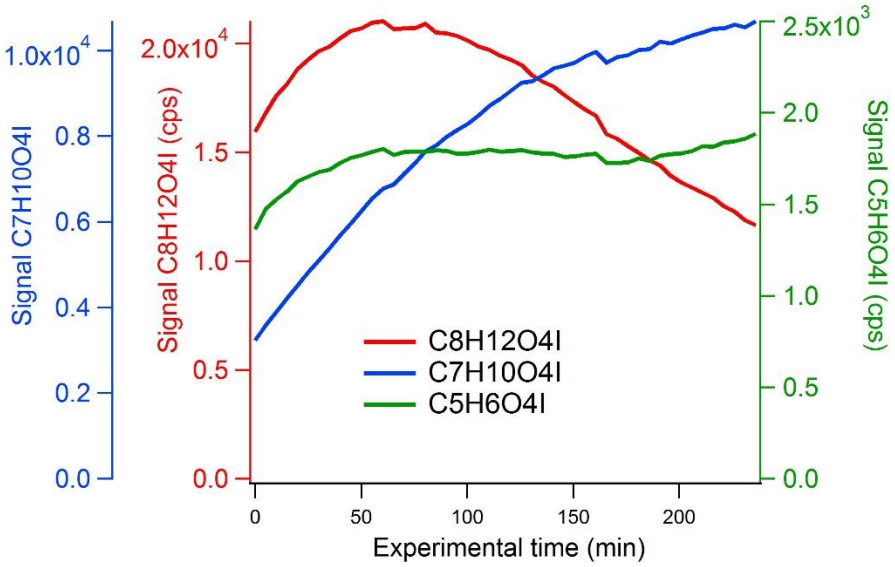

Figure S8: The temporal profiles of the three monomeric products determined from the three case studies (Figure S7). The high mass resolution data of their iodide clusters are presented. The color coding of these compounds matches that used in Figure S7.

S3.3. Functionalization Reactions of Dimers

While the majority of dimer signals decayed monotonically, a total of 12 mass spectral signals in the dimer region (iodide experiment) exhibited a temporary increase, followed by decay. These signals and their temporal evolution are shown in Figure S9.

There are three potential explanations for the temporary formation of dimers.

1: Formation of dimers via radical-radical recombination.

It has been shown that aqueous-phase OH oxidation of monomers can give rise to dimers and oligomers through radical-radical chemistry.[10–12] However, such reactions are more likely when the organic concentration is at the mM level or higher. Assuming an average molecular weight of 200 g mol^{-1} for the α-pinene SOA component, the total organic concentration is at most 0.7 mM in our experiments. The concentration of each individual compound is much lower. Under such dilute conditions, the radical-radical chemistry is unlikely to be important.

2: Formation of dimers from fragmentation of trimers.

We did not observe any trimers using the current technique. However, the presence of trimers or higher oligomers cannot be ruled out, as these low-volatile compounds may not evaporate in the thermal-desorption line of Aerosol-CIMS. Currently, we do not have a means to examine this possibility.

3: Functionalization of dimers.

It's been shown by our previous work[13] that the aqueous-phase OH oxidation is accompanied by an efficient conversion of a hydroxyl functional group to a carbonyl group, and a carbonyl group (aldehyde) to a carboxylic acid. Such functionalization reactions are the most likely explanation for the temporary formation of certain dimer signals.

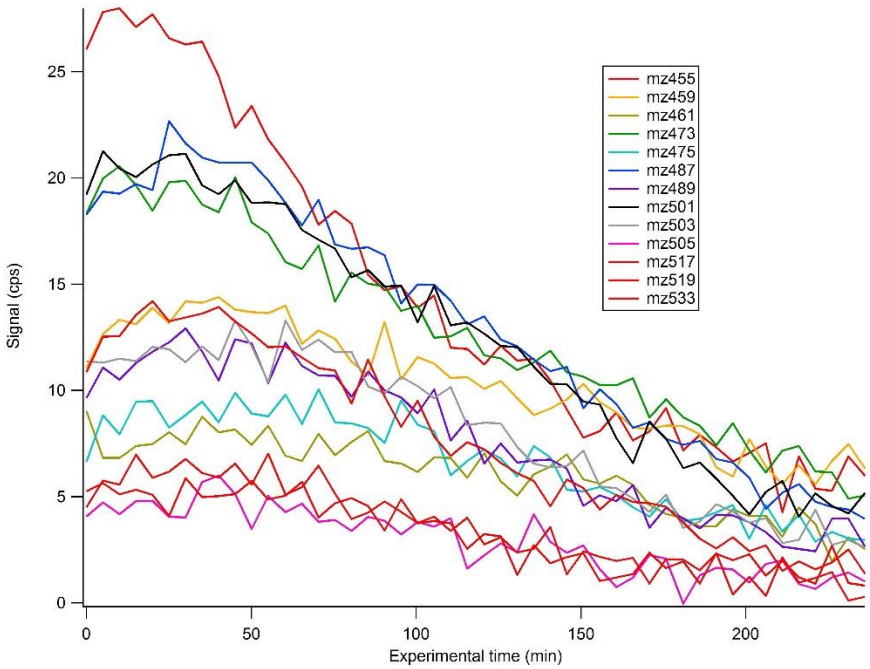

Figure 9: The unit mass resolution signals of dimers exhibited a temporary increase during the iodide OH oxidation experiment. The m/z are the iodide clusters of these compounds.

S4. H_2O_2 Control Experiment (Direct Photolysis)

A control experiment with no H_2O_2 added was performed for each reagent ion to assess the relative contribution of direct photolysis to the dimers. The total dimer signal is obtained by summing unit mass resolution (UMR) peaks in the same dimer regions as defined in the OH-oxidation experiments. The change of the total dimer signal during the H_2O_2 control experiments are compared with the signal change of pinonic acid (PIN) to estimate the direct photolysis rate of the total dimer (J_{dimer}).

S4.1. Estimation of PIN photolysis rate in the photo-reactor

The PIN photolysis rate (J_{PIN}) in the UVB photo-reactor employed in this study is calculated according to Eqn S1:

$$J_{PIN} = \int f(\lambda)\sigma(\lambda)\phi(\lambda)d\lambda \approx \sum f(\lambda)\sigma(\lambda)\phi(\lambda) \qquad \text{(S1)}$$

where the photon flux of the UVB photo-reactor ($f(\lambda)$) has been determined in our previous studies,[14] the absorption coefficient ($\sigma(\lambda)$) and quantum yield ($\varphi(\lambda)$) of PIN in the aqueous phase have been reported by Lignell et al.[15] The quantum yield of PIN is recommended to be independent of wavelength at this range, with a constant value of 0.5.[15] The photon flux, absorption cross section and the action spectra (wavelength-dependent J_{PIN}) are summarized in Figure S10. The J_{PIN} value is equivalent to the area under the action spectra and is calculated to be 2.9×10^{-5} s^{-1}.

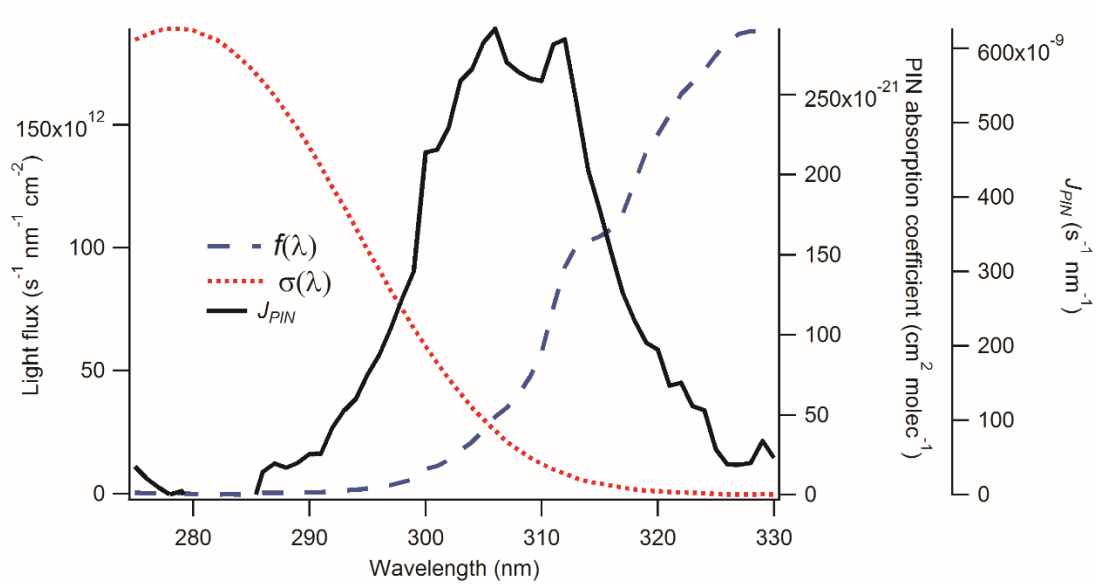

Figure S10: The UVB photon flux ($f(\lambda)$), PIN absorption cross section ($\sigma(\lambda)$) and the action spectra (J_{PIN}) in the current system.

S4.2. Comparison of J_{PIN} and J_{dimer}

As mentioned in the main article, the instability of the atomizer renders the quantification of J_{dimer} values difficult. The signals from certain experiments exhibited an increase during the H_2O_2 control experiments, perhaps due to the increase in the atomizer output. We did not use a scanning mobility particle sizer (SMPS) to monitor the atomizer output in all the experiments, making it difficult to correct the signal to

the total amount of particles generated by the atomizer. Here we compare the observed decay of the total dimers with that of the PIN signal for a rough estimation of J_{dimer}, assuming that the total dimer and PIN signals are equally affected by the atomizer output.

The decay of the total dimer signal and PIN are averaged across the three H_2O_2 control experiments using the three reagent ions. The first order decay plot of the averaged total dimer signal and PIN signal are shown in Figure S11. The observed J_{PIN} derived from Figure S11, 3.5×10^{-5} s^{-1} agrees well with the calculated J_{PIN} (2.9×10^{-5} s^{-1}). In average, the total dimer decays at a rate that appears to be 7.2 times smaller than that of PIN.

S4.3. Estimation of the contribution of J_{dimer}

Using the calculated J_{PIN} value and the observed ratio of J_{PIN} to J_{dimer}, the J_{dimer} is roughly at 4×10^{-6} s^{-1}. This value is a few percent of the pseudo-1st order decay of dimer ($k^{I}{}'_{dimer}$) observed in OH-oxidation experiment, indicating that direct photolysis of the total dimer is negligible.

However, there are uncertainties in this analysis. First, the decay of dimers and PIN during the H_2O_2 control experiments may not be solely due to direct photolysis but also due to radical chemistry. Our previous study has shown that the water soluble organic compounds (WSOC) of SOA generated from α-pinene ozonolysis gave rise to OH radical upon irradiation with UVB lights. More recently, Tong et al.[16] have proposed OH radical formation via hydrolysis of organic peroxide in WSOC. Second, the three H_2O_2 control experiments showed significant variation. The J_{dimer} value obtained in this work should be viewed as a reference under a specific reaction condition. Future studies should investigate the direct photolysis of dimers and other highly oxygenated organic compounds in more details.

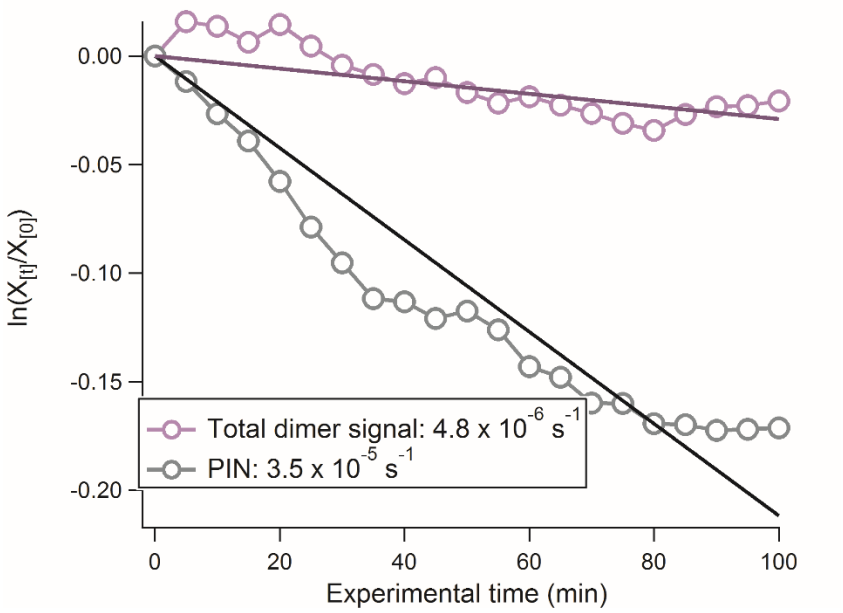

Figure S11: The 1st-order decay plot of the total dimer signal and PIN signal averaged across the three H_2O_2 control experiments. The 1st-order decay rates are shown in the dialogue box.

References

(1) Zhang, Q.; Jimenez, J. L.; Canagaratna, M. R.; Ulbrich, I. M.; Ng, N. L.; Worsnop, D. R.; Sun, Y. Understanding atmospheric organic aerosols via factor analysis of aerosol mass spectrometry: a review. *Anal. Bioanal. Chem.* **2011**, *401*, 3045–3067.

(2) Craven, J. S.; Yee, L. D.; Ng, N. L.; Canagaratna, M. R.; Loza, C. L.; Schilling, K. A.; Yatavelli, R. L. N.; Thornton, J. A.; Ziemann, P. J.; Flagan, R. C.; et al. Analysis of secondary organic aerosol formation and aging using positive matrix factorization of high-resolution aerosol mass spectra: application to the dodecane low-NOx system. *Atmos. Chem. Phys.* **2012**, *12*, 11795–11817.

(3) Lopez-Hilfiker, F. D.; Lee, B. H.; D'Ambro, E. L.; Thornton, J. A. Constraining the sensitivity of iodide adduct chemical ionization mass spectrometry to multifunctional organic molecules using the collision limit and thermodynamic stability of iodide ion adducts. *Atmos. Meas. Tech.* **2016**, *9*, 1505.

(4) Kanakidou, M.; Seinfeld, J. H.; Pandis, S. N.; Barnes, I.; Dentener, F. J.; Facchini, M. C.; Van Dingenen, R.; Ervens, B.; Nenes, A.; Nielsen, C. J.; et al. Organic aerosol and global climate modelling: a review. *Atmos. Chem. Phys.* **2005**, *5*, 1053–1123.

(5) Canagaratna, M. R.; Jayne, J. T.; Jimenez, J. L.; Allan, J. D.; Alfarra, M. R.; Zhang, Q.; Onasch, T. B.; Drewnick, F.; Coe, H.; Middlebrook, A.; et al. Chemical and microphysical characterization of ambient aerosols with the aerodyne aerosol mass spectrometer. *Mass Spectrom. Rev.* **2007**, *26*, 185–222.

(6) Aljawhary, D.; Lee, A. K. Y.; Abbatt, J. P. D. High-resolution chemical ionization mass spectrometry (ToF-CIMS): application to study SOA composition and processing. *Atmos. Meas. Tech.* **2013**, *6*, 3211–3224.

(7) Monod, A.; Doussin, J. Structure-activity relationship for the estimation of OH-oxidation rate constants of aliphatic organic compounds in the aqueous phase: alkanes, alcohols, organic acids and bases. *Atmos. Environ.* **2008**, *42*, 7611–7622.

(8) Doussin, J.-F.; Monod, A. Structure-activity relationship for the estimation of OH-oxidation rate constants of carbonyl compounds in the aqueous phase. *Atmos. Chem. Phys.* **2013**, *13*, 11625–11641.

(9) Beck, M.; Hoffmann, T. A detailed MS n study for the molecular identification of a dimer formed from oxidation of pinene. *Atmos. Environ.* **2016**, *130*, 120–126.

(10) Lim, Y. B.; Tan, Y.; Perri, M. J.; Seitzinger, S. P.; Turpin, B. J. Aqueous chemistry and its role in secondary organic aerosol (SOA) formation. *Atmos. Chem. Phys.* **2010**, *10*, 10521–10539.

(11) Renard, P.; Siekmann, F.; Gandolfo, A.; Socorro, J.; Salque, G.; Ravier, S.; Quivet, E.; Clement, J.-L.; Traikia, M.; Delort, A.-M.; et al. Radical mechanisms of methyl vinyl ketone oligomerization through aqueous phase OH-oxidation: on the paradoxical role of dissolved molecular oxygen. *Atmos. Chem. Phys.* **2013**, *13*, 6473–6491.

(12) Ervens, B.; Renard, P.; Tlili, S.; Ravier, S.; Clément, J.-L.; Monod, A. Aqueous-phase oligomerization of methyl vinyl ketone through photooxidation – Part 2: Development of the chemical mechanism and atmospheric implications. *Atmos. Chem. Phys* **2015**, *15*, 9109–9127.

(13) Zhao, R.; Mungall, E. L.; Lee, A. K.; Aljawhary, D.; Abbatt, J. P. Aqueous-phase photooxidation of levoglucosan–a mechanistic study using aerosol time-of-flight chemical ionization mass spectrometry (Aerosol ToF-CIMS). *Atmos. Chem. Phys.* **2014**, *14*, 9695–9706.

(14) Badali, K. M.; Zhou, S.; Aljawhary, D.; Antiñolo, M.; Chen, W. J.; Lok, A.; Mungall, E.; Wong, J. P. S.; Zhao, R.; Abbatt, J. P. D. Formation of hydroxyl radicals from photolysis of secondary organic aerosol material. *Atmos. Chem. Phys.* **2015**, *15*, 7831–7840.

(15) Lignell, H.; Epstein, S. A.; Marvin, M. R.; Shemesh, D.; Gerber, B.; Nizkorodov, S. Experimental and Theoretical Study of Aqueous cis-Pinonic Acid Photolysis. *J. Phys. Chem. A* **2013**, *117*, 12930–12945.

(16) Tong, H.; Arangio, A. M.; Lakey, P. S. J.; Berkemeier, T.; Liu, F.; Kampf, C. J.; Brune, W. H.; Pöschl, U.; Shiraiwa, M. Hydroxyl radicals from secondary organic aerosol decomposition in water. *Atmos. Chem. Phys.* **2016**, *16*, 1761–1771.